Saudi Pharmaceutical Journal (2017) **25**, 346–358

King Saud University

Saudi Pharmaceutical Journal

www.ksu.edu.sa
www.sciencedirect.com

ORIGINAL ARTICLE

Direct and enhanced delivery of nanoliposomes of anti schizophrenic agent to the brain through nasal route

Pratik Upadhyay [a,*], **Jatin Trivedi** [a], **Kilambi Pundarikakshudu** [a], **Navin Sheth** [b]

[a] *Department of Pharmaceutical Technology, L. J. Institute of Pharmacy, Ahmedabad, Gujarat, India*
[b] *Department of Pharmaceutical Sciences, Saurashtra University, Rajkot, Gujarat, India*

Received 16 November 2015; accepted 25 July 2016
Available online 5 August 2016

KEYWORDS

Nasal route;
Dispersion;
Blood brain barrier;
Liposomes;
Quetiapine Fumarate

Abstract The problem of inadequate oral bioavailability of Quetiapine Fumarate, a lipophilic drug used for schizophrenia, due to hepatic metabolism and repulsion by brain barrier was attempted in this study. Combination of two approaches, viz. Quetiapine inclusion into the liposomal carrier for better diffusion and administration through nasal route to avoid hepatic metabolism and barrier elimination was applied. Thin film hydration followed by sonication method was employed in liposome preparation and the formulation was optimized using 3^2 full factorial design. The number of sonication cycles (X_1) of 2 min and 80% amplitude and molar ratio of constructional components such as cholesterol to egg phosphatidylcholine (X_2) as independent variables and a % of entrapment efficiency (Y_1) and cumulative *in vitro* drug release (Y_2) at 6 h as dependent variables was selected. Batch F7 prepared by 2 cycles of sonication and 1:3 M ratio of cholesterol: egg phosphatidylcholine was optimized as a consequence of substantial entrapment efficiency of 75.63 ± 3.77%, and 99.92 ± 1.88% drug release and 32.33 ± 1.53% drug diffusion, which was optimum among all other batches at 6 h. Diffusion study was done for all the batches of liposomal formulation by using sheep nasal mucosa and good amount with better diffusion rate was measured which proved liposomal dispersion a virtuous delivery system for brain drug delivery through nasal route. Results of *in vivo*, ciliotoxicity and gamma scintigraphy studies on mice supported the above inference.

* Corresponding author at: Department of Pharmaceutical Technology, L. J. Institute of Pharmacy, L. J. Campus, Between Kataria Motors and Sarkhej Circle, Off. Sarkhej–Gandhinagar Road, Ahmedabad 382 210, Gujarat, India.
E-mail address: pratik_pharmacist@yahoo.com (P. Upadhyay).
Peer review under responsibility of King Saud University.

Production and hosting by Elsevier

http://dx.doi.org/10.1016/j.jsps.2016.07.003
1319-0164

1. Introduction

Schizophrenia is a disorder of brain and characterized by the sudden breakdown of thought processes and by poor emotional responses. In contrast to other tissues, brain endothelial cells are more intimately associated and that prevent access of any potentially toxic substances into the brain (Pardridge, 1999). Any molecule enters through the blood into the brain is restricted by this barrier made up of endothelial cells' "Tight Junctions" or "*Zonula Occludens*" or also called as blood brain barrier (BBB) (Misra et al., 2003). Owing to its stringent penetrability, it is presumed to be the key obstacle in the development of central nervous system (CNS) targeted drug delivery (Pathan et al., 2009). Various strategies to use different routes of drug administration than oral or parenteral route such as intranasal and olfactory route and like to use drug nanocarriers have been applied to cope with the problem of the transportation across the blood brain barrier (Abbott and Romero, 1996).

The historical backdrop of nasal drug transportation goes once again to prior topical applications of medications proposed for local effects (Alsarra et al., 2010). Intranasal drug delivery has numerous focal compensation over other routes of drug administration (Behl et al., 1998; Costantino et al., 2007; Illum, 2000). Late improvements in nasal drug delivery have recommended intranasal administration as a safe and adequate course for brain targeting, especially for drugs with biological consequences on the CNS and constrained BBB permeability (Watts et al., 2002). The Olfactory region is of significant interest toward medication conveyance in light of the fact that it evades the BBB, conveying restorative drugs to the CNS (Frey, 2002). Nasal delivery is easily accessible, convenient, and a dependable system, with a porous endothelial membrane, and a profoundly vascularized epithelium that provides a quick assimilation of the compound into the systemic circulation, circumventing the hepatic first pass disposal (Parmar et al., 2011; Türker et al., 2004). In addition to that, intranasal drug delivery enables reduction in the dose, quick therapeutic level attainment of the drug into the blood, speedier onset of pharmacological activity, and fewer side effects (Arora et al., 2002; Ugwoke et al., 2001). It is reported that lipophilic drugs are by and large, well absorbed from the nasal cavity with pharmacokinetic profiles, which are frequently indistinguishable to those acquired after an intravenous infusion with a bioavailability approaching 100% (Aacharya et al., 2015). Strategy of delivering the drug by intranasal route could be effective in the delivery of therapeutic proteins such as brain delivered neurotropic factor (BDNF) to the olfactory bulb as a treatment for Alzheimer's disease (Thorne et al., 1995).

Colloidal drug transporters resembling micelles, emulsions, liposomes and nanoparticles have been largely accounted for brain drug delivery because methods of preparation are generally simple and easy to scale-up (Garcia et al., 2005; Woensel et al., 2013). Liposomes are self-assembling colloidal structures comprising of lipid bilayers encompassing an aqueous compartment, and can typify the wide range of hydrophilic drugs within this compartment (Pathan et al., 2009). Liposomes have been demonstrated to provide stable epitome to different drugs and offer unique focal points over un-encapsulated agents (Lasic and Papahadjopoulos, 1995).

Thus, liposomes have been proposed for utilization in an assortment of applications in research, industry, and medicine, especially for the utilization as transporters of symptomatic and therapeutic compounds (Fang et al., 2009). The unique ability of liposomes to entrap drugs, in both an aqueous and a lipid phase makes such delivery systems attractive for hydrophobic and hydrophilic drugs, such encapsulation proved to reduce drug toxicity while retaining or improving the therapeutic adequacy (Fielding, 1991). Liposomes are most commonly used carrier of mixes for brain delivery *in vivo* (Afergan et al., 2008; Schnyder et al., 2005; Shi et al., 2001; Xie et al., 2005) and proved to enhance bioavailability of numerous deprived agents into the brain (Alsarra et al., 2008; Arumugam et al., 2008; Hamed et al., 2012; Vyas et al., 1995).

Quetiapine Fumarate (QTF) is indicated for the treatment of schizophrenia and also for the acute manic episodes associated with bipolar I disorder. QTF is an antipsychotic drug with limited oral bioavailability (7–9%) due to hepatic metabolism and excision by the blood brain barrier (Brayfield and Sweetman, 2007). Albeit numerous endeavors have been made to attain brain entry of QTF, it doesn't efficiently infiltrate into the BBB (Kararli et al., 1992; Lohan et al., 2015).

It was hypothesized that if saline liposomal suspension of QTF administered through nasal route, it would avoid hepatic first pass metabolism and BBB crossover, and hence could achieve improved bioavailability and brain targeted drug delivery. The objective of the present study was to formulate different factorial batches of QTF liposomes by varying the molar ratio of constructional components and optimize by comparison for % entrapment efficiency and % drug release with time. The applied factorial design was validated and all the batches were further evaluated for diffusion through the sheep nasal mucosa by *ex vivo*. The optimized batch was then radiolabeled and compared with the simple solution of ^{99m}Tc in simulated nasal fluid (SNF) using a gamma scintigraphy study, which is then sustained by comparison of liposomal dispersion with the simple dispersion of QTF by *in vivo* study in mice.

2. Materials and method

2.1. Materials

QTF was a generous gift from Elite pharmaceuticals, Ahmedabad. Egg Phosphatidylcholine (EPC) was obtained as a gift sample from Vav Life sciences Pvt. Ltd., Mumbai, and Cholesterol (CH) was purchased from Astron Chemicals, Ahmedabad.

2.2. Analytical method

QTF is analyzed for %EE, %CDR and % diffusion study by Uv double beam spectrophotometer (Shimadzu-1800, Japan) in SNF, pH 6.8 by generating standard curve for the entire range from 5 to 25 μg/ml at 242 nm (Sahu and Rana, 2011; Vincenzo et al., 2003). The method used for estimation of QTF in brain homogenate and plasma involves high performance liquid chromatography (HPLC) analysis (Model LC) using a C18 column with Uv detector. Mobile phase consists of phosphate buffer (pH 3): Acetonitrile: Methanol

(50:40:10) and flow rate were 0.8 ml/min. The sample volume injected is 20 µl and wavelength was 247 nm (Reddy et al., 2011).

2.3. Preparation of liposomes

Liposomes of QTF were prepared by modifying thin lipid film hydration technique using a rotary flask evaporator as described by the method of Bangham, Juliano and Daoud (Senthilkumar et al., 2012). Process parameters such as solvent system, rehydration volume, vacuum, drying and hydration time, temperature and flask rotation speed were optimized on the basis of morphology of the film formed and particle size distribution by preliminary screening. These all the factors were analyzed for their effects on the blank liposome formation. The effect of one variable was studied at a time, keeping other variables constant. Amount of drug was screened at last (Rathod and Deshpande, 2010; Shariat et al., 2014).

In the first step of the preparation, CH: EPC in the different molar ratio and 38.35 mg of QTF (molar ratio of 1) was dissolved in 10 ml of methanol: chloroform solution of 2:1 ratio. The flask was attached to the rotary evaporator and rotated at 90 rpm speed for 120 min at 37 °C temperature (T_m of EPC) under vacuum (600 mmHg). Our preliminary study findings showed that liposome size, zeta potential and drug leaching are lowered at reduced temperature, which reflects in more percentage liposomal yield and higher drug entrapment while drying time is oppositely increased. The organic solvent was slowly removed by this process such that a very thin, smooth and dry film of lipid was formed on the inner surface of the flask. The film was allowed to dry for 1 h under vacuum and temperature previously mentioned. The dry lipid film was then slowly hydrated with an aqueous phase (10 ml SNF, pH 6.8) and the flask was again rotated at the same speed for 30 min at 37 °C. Liposomal dispersion was left to mature overnight just below 20 °C to ensure full lipid hydration. The liposomal dispersion obtained was filled in glass ampoules and sonicated for 2 min at 80% amplitude and then was subjected to centrifugation at 5000 rpm, 8 °C for 5 min using Remi ultracentrifuge. Liposomal suspension was separated from drug and debris pellet and stored in refrigerator (Liu et al., 2013).

Here, the drug is water insoluble so it will not be in a molecular state and free drug will separate at lower rpm. Similarly, insoluble fragments and crystals of cholesterol and the EPC will settle down in form of pellets. The number of sonication cycles was varied from 2 to 4 times. The time was fixed for only 2 min as above that liposomal dispersion starts getting heat and drug leaches out which results into deprived entrapment efficiency. The amplitude of sonication was kept 80% as it increases sonochemical effect which results in the fine particle formation (Santos and Lodeiro, 2009).

2.4. Experimental design

A 3^2 full factorial design was utilized in the present study (Ghanbarzadeh et al., 2013). Several studies revealed that the ratio of CH: EPC plays notable role in lamellar configuration and sonication plays important role in structure type of the Liposomes (Nill, 2003; Joseph and Zasadzinski, 1986). These both effects fall out significant impact on entrapment of the drug and release of the drug from liposomal lamella (Hiromasa et al., 1999; Briuglia et al., 2015). In this design two factors were evaluated, each at three levels, and experimental trials were carried out at all nine possible combinations. The design layouts and coded value of independent factor are shown in Table 1. The molar ratio of CH: EPC and the number of sonication cycles of 2 min and 80% amplitude were selected as independent variables. The % entrapment efficiency and % cumulative drug release (%CDR) of QTF were selected as dependent variables.

2.5. Characterization and evaluation

2.5.1. Drug - excipient compatibility study

The compatibility study was carried out by using Fourier transform infrared spectroscopy (FTIR) (MIRacle-10, Shimadzu, Japan) (Pavia et al., 2008). The physical mixtures of 1:1 were prepared for QTF and egg lecithin, drug and physical mixture (cholesterol and egg lecithin) and also for egg lecithin and individual dry ingredients of the simulated nasal fluid that is potassium chloride (KCl), sodium chloride (NaCl) and calcium chloride ($CaCl_2$). These mixtures were kept for one month at room temperature that is 25 °C ± 2 °C and 60% ± 5% relative humidity for complete interaction between the drug and polymer. The drug and drug-polymer samples were dried in hot air oven at 60 °C for 30 min for removal of moisture. These samples were scanned from 4000 to 400 cm^{-1} wave numbers. Spectra obtained were compared with spectra of QTF sample for changes in the peaks if any interaction transpires.

2.5.2. Microscopy

Morphology of liposomes was studied under microscope. All batches of the liposomes prepared were viewed under an Olympus binocular microscope with camera attachment having an S-Viewer version 1.10.6.2 software to study their shape. The liposomal dispersion was suitably diluted and put on a glass slide and viewed with a binocular microscope with magnification of 15 × 100. Scanning electron microscopy (SEM) and transmission electron microscopy (TEM) of the optimized liposomal formulation were performed for determining the surface morphology, size and shape of the formulation and observing the aggregation property of liposomes.

Table 1 Formulation design with coded values.

CH:EPC (X_2)		Sonication cycles (2 min. 80% amp.) (X_1)		Batch
Coded value	Molar ratio	Coded value	Cycles	
−1	1:1	−1	2	F1
		0	3	F2
		+1	4	F3
0	1:2	−1	2	F4
		0	3	F5
		+1	4	F6
+1	1:3	−1	2	F7
		0	3	F8
		+1	4	F9

2.5.3. Particle size and surface charge

The particle size and size distribution of liposomes were determined by Malvern zetasizer based on laser light scattering principle. A Malvern laser light scattering zetasizer equipped with an argon laser was utilized for evaluating the particle size and size distribution. Light scattering was monitored at 90° angle and at 25 °C. The mean droplet size was calculated from intensity, volume and bimodal distribution assuming spherical particles. The zeta potential is an indication of the stability of the colloidal systems and indicates charge present in the colloidal systems. Zeta potential of formulations was determined using Malvern zetasizer. Samples were placed in clear disposable zeta cells and results were recorded.

2.6. Ex vivo drug diffusion study

An *ex vivo* diffusion study was carried out using freshly derived sheep nasal mucosal epithelium from slaughter house (Lohan et al., 2015; Aacharya et al., 2015). Mucosal membrane (0.2 mm thick, 10 mm diameter and 78.5 mm^2 area) was fixed in between receptor and donor compartment of the Franz diffusion cell. 9 sets of cells were used for all the formulations of liposomal dispersion of QTF. Acceptor compartment was filled with 10 ml SNF, pH 6.8 and donor compartment was filled with 1 ml 5% w/v dispersion. All the nine experimental batches were tested for the *ex vivo* drug diffusion study and total amount of the drug content in the dispersion taken for the study was calculated considering the entrapment efficiency of individual batch. The temperature in diffusion chamber was maintained at 37 °C using thermostatic water bath. The sample was withdrawn at time 1, 2, 3, 4, 5 and 6 h and fresh SNF was added to make the volume. The samples were filtered through 0.45 μm nylon filter membrane and analyzed using spectrophotometer for drug content at 242 nm. Results were expressed as an amount permeated or percent diffusion or ex vivo brain availability as Eq. (1) as follows:

$$\%\ Diffusion = Ap \times 100/At \quad (1)$$

Ap = amount of QTF in receptor compartment.
At = Initial amount of QTF in donor compartment.

2.7. Optimization

2.7.1. %Entrapment efficiency

The entrapment efficiency was determined by the solvent sonication method (Brgles et al., 2008; Tomoko and Fumiyoshi, 2005). Briefly, the vesicles were broken by dissolving 1 g liposomes (equivalent to 167.8 mg QTF) into 10 ml methanol (theoretical yield 16.78 mg/ml) and sonicated for 5 min to release the drug, which was then estimated for the drug content by diluting up to 100 times (Laouini et al., 2012). The percent drug entrapped (PDE) was then calculated using the following Eq. (2).

$$\%Entrapment\ efficiency = Entrapped\ drug \times 100/Total\ drug\ added \quad (2)$$

2.7.2. In vitro drug release (%CDR)

Studies of the drug release from all the prepared liposomal batches were directed toward the approaches that are relevant to the *in vivo* condition. The *in vitro* release studies of QTF from the liposomal dispersion was studied through the dialysis membrane bag (10 KDa molecular weight, Himedia) in a glass beaker containing 100 ml of SNF (pH 6.8) at 37 °C ± 0.5 °C on a temperature controlled magnetic stirrer (Arumugam et al., 2008; Jung et al., 2009). Dialysis membrane tube previously soaked overnight in the ethanol was filled with 5 ml of SNF containing 1 g liposomes. 1 ml volume was withdrawn at the interval of every 30 min up till 6 h and fresh SNF was added to make the volume. The samples were diluted with dissolution medium and analyzed for drug content.

2.7.3. Regression statistics and analysis of variance (ANOVA)

Application of regression analysis is important to check that our independent variables have a significant effect on our response or not. Application of regression also gives us an idea about the effect of the interaction of both independent variables on the dependent variable. All data derived from both the responses were evaluated statistically for their correlation by regression and ANOVA.

2.7.4. Polynomial equation generation and reduction

The polynomial equations can be used to draw conclusions after considering the magnitude of coefficient and the mathematical sign it carries (i.e. positive or negative). The equations may be used to obtain the estimates of response as a small error of the variance was noticed in three replicates. Reduction in the equation is based on the significance value, and those terms are removed, which are insignificant ($P > 0.05$).

$$Y_1 = b_0 + b_1X_1 + b_2X_2 + b_1^2X_1^2 + b_2^2X_2^2 + b_{12}X_1X_2 \quad (3)$$

Eq. (3), Y_1 = Encapsulation efficiency,
And,

$$Y_2 = b_0 + b_1X_1 + b_2X_2 + b_1^2X_1^2 + b_2^2X_2^2 + b_{12}X_1X_2 \quad (4)$$

Eq. (4), Y_2 = %cumulative drug release

b_0 = arithmetic mean response of the nine runs,
X_1 = Ratio of CH: EPC and X_2 = sonication cycles.

2.7.5. Validation of mathematical model

To evaluate the reliability of the developed mathematical model, all the values of batches for prediction and actual are compared and residuals are measured. The responses of optimized batch and modified optimized batch are compared. They are estimated by use of generating a model covering the entire experimental domain again, residuals versus practical runs are plotted to check the variation from center line of each run and predicted value was compared with practical value and checked for residual. Two checkpoint batches were prepared, keeping one independent variable constant at one time and another was slightly fluctuated from standard value. Practical value was checked for the impact of fluctuated independent variables on the dependent variable for which it contributes more.

So, accordingly first checkpoint batch was prepared by fluctuating sonication cycle timing and checked for residual difference in entrapment efficiency of practical with the predicted value of the standard one (optimized batch for entrapment efficiency). Similarly, the second checkpoint batch was prepared by fluctuating molar ratio of CH: EPC and checked for residual difference in % of drug release of practical with the predicted value of the standard one (optimized batch for % drug release).

2.8. Release kinetic studies – release pattern and mechanism

There are several linear and nonlinear kinetic models widely used to describe release patterns and mechanisms from various systems and to compare test and reference dissolution profiles. Linear models include zero order, Higuchi, Hixson-Crowell and polynomials, whereas the nonlinear models include first order, Weibull, Korsmeyer-Peppas. The model dependent methods all rely upon a curve fitting procedure. The method of Bamba (Bamba et al., 1979) was adopted for deciding the most appropriate model.

2.9. Animal study

2.9.1. Gamma scintigraphy

All the animal studies were properly designed and performed, which were reviewed and approved by an institutional animal ethics committee. For ^{99m}Tc labeled solution, 0.4 ml of SNF pH 6.8 solution was injected into a 10 ml sterile vacuum vial. A newly prepared solution of $SnCl_2{\cdot}H_2O$ 0.5 ml was added, immediately followed by the addition of 0.1 ml of elute containing 1 mCi ^{99m}Tc in the form of sodium pertechnetate ($NaTcO_4$). The mixture was heated for 10 min in a boiling water bath, and then cooled to room temperature.

For ^{99m}Tc labeled liposomal dispersion, above prepared solution is added in thin film formed in a round flask at the stage of rehydration instead of SNF pH 6.8. After rehydration of lipid film by a solution of sodium pertechnetate, sonication was done to reduce size of lamella. Liposomes were separated by centrifugation, and redispersed by the addition of SNF pH 6.8. The entrapment efficiency of liposome for the ^{99m}Tc was measured 58.6 ± 7.5% by gamma particle count up to 1000. After 2 h it was measured 48.1 ± 6.2 indicated that liposomal ^{99m}Tc is significantly more stable.

Albino mice weighing 20–25 g were used after overnight fasting. Two mice were employed in the study. 10 µl liposomal dispersion containing Technetium^{99m} (equivalent to 250 µCi) in SNF pH 6.8 (equivalent to 12 mCi/kg body weight) was administered intranasally to the first mouse while in the second mouse SNF pH 6.8 solution containing ^{99m}Tc was administered intranasally of same strength. Dose for mice was calculated by the same method described for *in vivo* study considering 1 mCi/kg dose of human (Hildebrandt et al., 2008). Gamma photomicrographs were developed at 1000 counts with GE Millennium VG Hawkeye Dual Head Nuclear Camera (Variable-Geometry Dual Detector Gamma Camera).

2.9.2. In vivo study

Albino mice weighing 20–25 g were used after overnight fasting. Human equivalent dose for mice was calculated by body surface area (Eq. (6)) as well as weight method (Eq. (7)) (Freireich, 1966). A general dose of 60 kg healthy human is 400 mg, so human equivalent dose (HED) is 6.67 mg/kg for healthy human weighing 60 kg. So,

$$\begin{aligned} \textit{Animal dose}\ (\text{mg/kg}) &= \textit{HED}\ (\text{mg/kg})/[\textit{Animal}\ \text{km}/\textit{Human}\ \text{km}] \\ &= 6.6666667/[3/37] \\ &= 6.6666667/0.0810810810811 \\ &= 82.222222\ (\text{mg/kg}). \end{aligned} \tag{5}$$

So, dose for mice weighing 20–25 g is ≈2 mg.
And,

$$\begin{aligned} \textit{Animal dose}\ (\text{mg/kg}) &= \textit{HED}\ (\text{mg/kg}) \times \textit{wt. factor} \\ &= 6.67 \times 12 = 80.00\ (\text{mg/kg}). \end{aligned} \tag{6}$$

So, dose for mice weighing 20–25 g is ≈2 mg.

Two groups of mice were employed in the study and all the readings were taken in triplicate (n = 3) for each time point. 10 µl QTF dispersion containing 2 mg QTF in SNF pH 6.8 was administered intranasally to the first group while in the second group QTF 10 µl liposomes containing 2 mg QTF was administered intranasally. For this study, mice were tied up in supine condition and nasal administration was done by micropipette. Mice were sacrificed after every 1 h interval of administration by stunning and blood was collected from carotid artery after decapitation and intact brains were excised from the skull and homogenized immediately at 5000 rpm for 10 min under chilled condition. Brain homogenate was made acidic by adding 1 ml of phosphate buffer (pH 3) and the drug was extracted twice times by adding mixture of 0.6 ml chloroform and 0.4 ml of methanol. The organic layer was separated after centrifugation at 5000 RPM for 10 min at 4 °C and evaporated under vacuum. The residue was resuspended in 1.6 ml acetonitrile and 0.4 ml HPLC grade methanol and then analyzed by HPLC method.

2.9.3. Nasal ciliotoxicity study

After diffusion study, nasal mucosa is unmounted from diffusion cell and stained with Safranin and eosin, and then analyzed under an Olympus microscope and compared with untreated nasal mucosal layer to check for any conformational changes.

3. Results and discussion

3.1. Analytical method

The Uv overlay absorption spectra were taken and the standard calibration curve was generated for the entire range from 5 to 25 µg/ml. Linearity was observed between 5 and 25 µg/ml at 242 nm in SNF pH 6.8. Equation Derived from Standard calibration curve is $y = 0.0079x - 0.005$ having value $R^2 = 0.9978$. Similarly, in HPLC method standard retention peak of the drug was observed at 5 min with peak area 1,195,711. Both the methods are indicated as shown in Fig. 1.

3.2. Characterization and evaluation

3.2.1. Drug - excipient compatibility study

FTIR spectra of alone QTF show its characteristic functional group peaks shown in Fig. 2 and QTF with the excipients

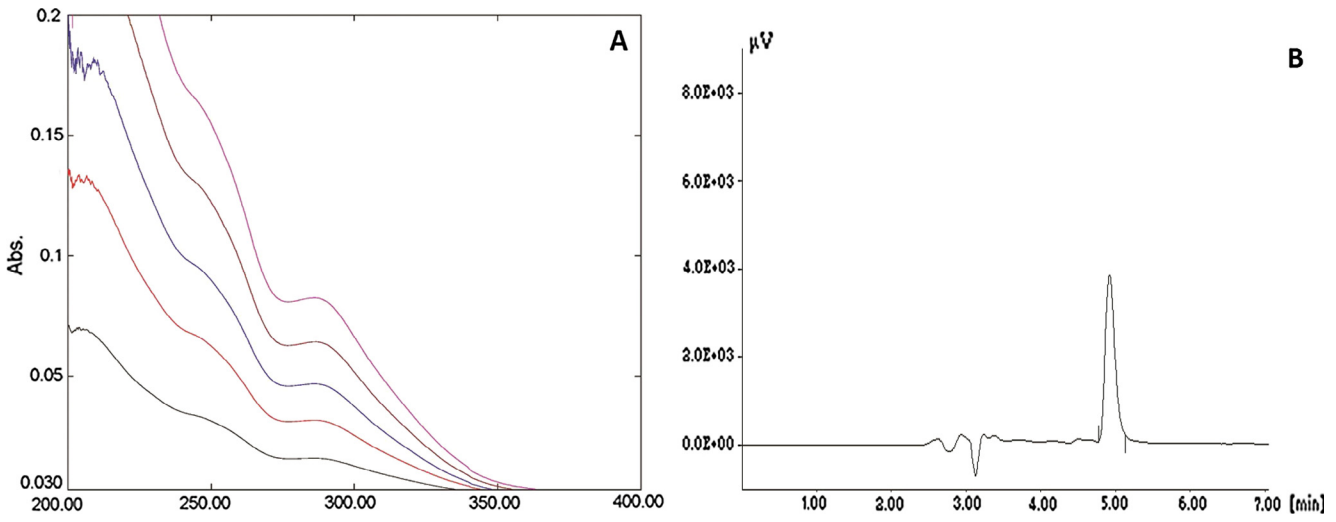

Figure 1 Analytical determination of QTF. A. Uv overlay absorption spectra of different dilutions of QTF; B. HPLC chromatogram of QTF.

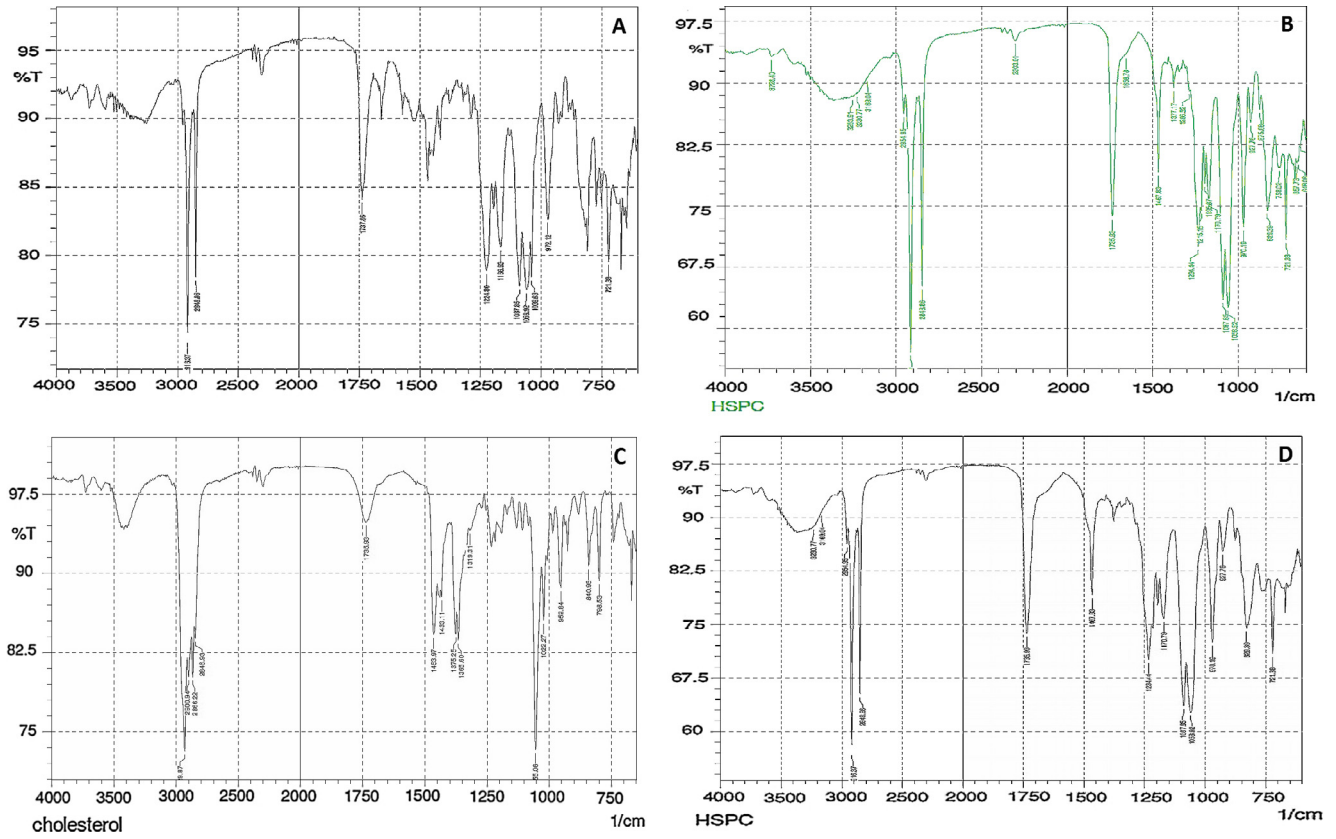

Figure 2 FTIR of. A. QTF pure; B. Mixture of QTF with excipient; C. Cholesterol; D. EPC.

shows almost same peak as the pure drug. Comparison of the peaks of the functional group obtained from QTF alone and QTF with excipients was done. In QTF with excipients spectra the fingerprint region and 4000–2000 cm^{-1} region show the peaks are identical to QTF functional groups as shown in Table 2. So, QTF is compatible with the excipients used in the formulation and no functional group loss or interaction of QTF with excipients was observed.

3.2.2. Microscopy

It can be stipulated from the photomicrograph that circular vesicles of phospholipid were formed. Scanning electron microscopy of the optimized liposomal formulation showed the intact, regular surface of completely dispersed liposomal spheres as shown in Fig. 3. From transmission electron microscopy, thick and rigid liposomal lamella has been identified.

3.2.3. Particle size

Average Particle size measured is 139.6 nm having intensity 100% and width 35.26 nm shown in Fig. 4. That means all the particles are within the range of 121.97 nm to 157.23 nm having a maximum accumulation at 139.6 nm. Here the zeta potential is −32.1 mV having intensity 100% and width 9.26 mV. That means all the particles are within the range of 27.47 mV to 36.73 mV having a maximum accumulation at −32.1 mV which indicates the system is moderately stable (Michel and Suzuki, 1985).

3.3. Ex vivo drug diffusion study

The drug diffusion was maximum of 59.02 ± 1.22 for formulation batch F7 containing 1:3 M ratio of cholesterol: EPC. Increasing the EPC content resulted in an increased drug release due to its bipolar nature which facilitates drug diffusion across biological membrane (Chandaroy et al., 2002). In Fig. 5 and Table 3, batch F7 also had a maximum release, which can be correlated with diffusion across a membrane by a concentration gradient.

3.4. Optimization

3.4.1. Entrapment efficiency

The maximum entrapment efficiency is observed in thrice time's ratio of EPC to cholesterol (Batch F4) among all other batches as shown in Fig. 6. This is due to the requirement of the abundant amount of EPC to make the lamellar structure of liposomes and cholesterol is supplement of lamella and increases stability as flexibility buffer. At an appropriate ratio of CH and EPC there is formation of rigid bilayers, which increases stability and entrapment efficiency of liposomes. Decrease in entrapment efficiency with increasing CH:EPC ratio at higher level is also observed, which is due to decrease in CH below certain concentration can disrupt the regular linear structure of liposomal membrane formed by EPC as a cause of instability. This may result in rupture of bilayers, which results in decreased entrapment efficiency.

Moreover, sonication cycles were applied to decrease the size of the liposomes formed at the last step of the formulation, which can result into the disruption of certain vesicles and hence decrease entrapment efficiency. From Table 4 it can be

Table 2 FTIR Analysis of drug and mixture.

Functional group	Standard frequency (cm^{-1})	Observed frequency of QTF (cm^{-1})	Observed frequency of mixture (cm^{-1})
C—H-Stretch mode	2962–2853	2920.23	2954.55
C═O-Stretch mode	1725–1705	1737.86	1735.5
N—H-Stretch mode	1575–1600	1541.12	1551.46
C═C-Stretch mode	1600–1690	1670.35	1676.15
C—N-Stretch mode	1250–1340	1375.26	1377.17
C—C-Stretch mode	1450–1600	1438.9	1465.9

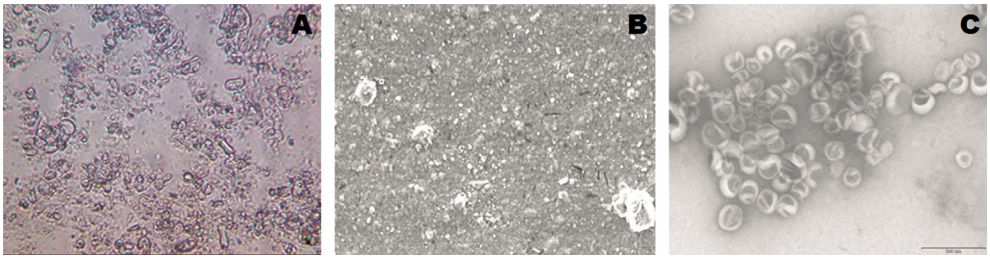

Figure 3 Microscopic images of liposomal formulation. A. Light microscope with magnification of 15 × 100; B. SEM (Scale: 1 cm = 100 nm); C. TEM (Scale: 1 cm = 100 nm).

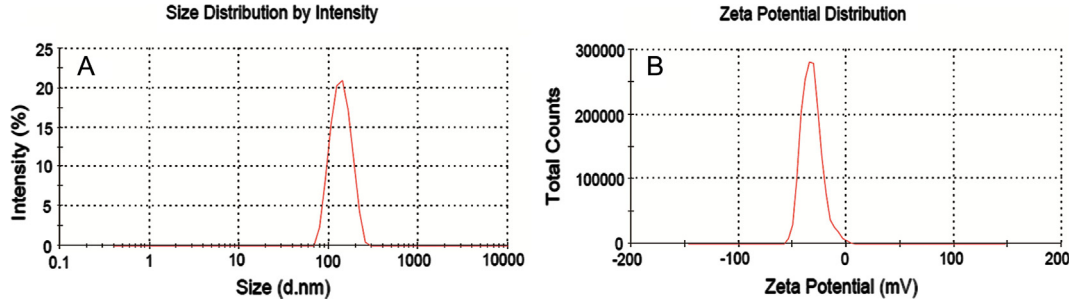

Figure 4 Zetasizer graph of optimized batch F7. A. Average particle size and size distribution measurement; B. Zeta potential determination.

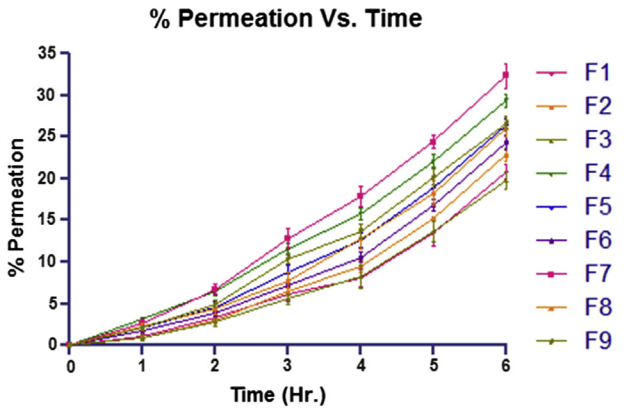

Figure 5 %Diffusion of liposomal dispersion (batches F1–F9) across sheep nasal mucosa with respect to time ($n = 3$).

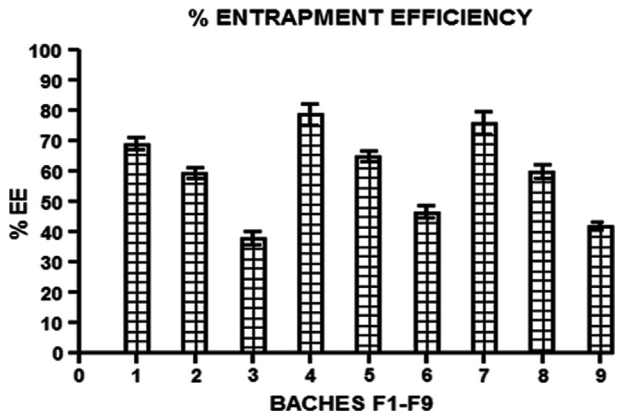

Figure 6 %Entrapment efficiency of all the batches (F1–F9) ($n = 3$).

stated that entrapment efficiency is maximum with least sonication cycles. Maximum entrapment efficiency was obtained with 1:2 (CH:EPC) molar ratio and 2 cycles of the sonication, so batch F4 is giving maximum entrapment efficiency of 78.66 ± 3.42.

3.4.1.1. Full model equation.

$$Y_1 = 65.33222 + 1.873333X_1 - 16.175X_2 - 3.09833X_1^2 - 5.95333X_2^2 - 0.6225X_1X_2 \quad (7)$$

The full model was evolved as in Eq. (8) and refined by excluding the terms for which the level of significance was greater than 0.05. The significant levels P of the coefficients b_0, b_1, b_2, b_{12}, b_{11} and b_{22} were found to be 0.0000164, 0.075085, 0.000177, 0.083318, 0.016121 and 0.519831 respectively. So, b_1, b_{12} and b_{11} have significance greater than 0.05, so they were omitted from the full model to generate a reduced model equation. The coefficients b_0, b_2, & b_{22} were found to be significant as $P < 0.05$; hence, they were retained in the reduced model.

3.4.1.2. Reduced model equation.

$$Y_1 = 65.33222 - 16.175X_2 - 5.95333X_2^2 \quad (8)$$

So, from Eq. (9) of the reduced model, it can be qualitatively concluded that X_2 (−16.175) had the negative effect on the response of Y_1, which indicated that as the number of sonication cycles increases, %EE decreases. The negative value of X_2^2 with significance above 99.95% indicates the number of sonication cycles has an inverse effect on %EE. Here, as the ratio of cholesterol to EPC increases, there is a slight increase in %EE as X_1 has positive value. Though it is insignificant, it is very close to significant value of 0.07. Moreover, its square is also very close to significant value. So, the X_1 has a minor positive effect on %EE (Y_1) means ratio itself as an X_1 contribute at smaller consent, and also at a very high level it decreases response Y_1. Higher values of correlation coefficient for % EE indicate a good fit.

3.4.2. In vitro drug release study

The drug release was maximum for formulation containing 1:3 M ratio of cholesterol: EPC. Increasing the EPC content resulted in a more drug release due to its bipolar nature which facilitates drug diffusion across lipid lamella as indicated in Fig. 7 and Table 5. Maximum drug release 99.920 ± 1.88 was observed with batch F7 at 6 h.

3.4.2.1. Full model equation.

$$Y_2 = 90.74633 + 5.983833X_1 - 3.26283X_2 + 0.1285X_1^2 + 0.2985X_2^2 + 0.75075X_1X_2 \quad (9)$$

The full model was evolved and refined by excluding the terms for which the level of significance was greater than 0.05 as per Eq. (10). The significant levels P of the coefficients b_0, b_1, b_2, b_{12}, b_{11} and b_{22} were found to be 0.000000602, 0.000342, 0.002057, 0.832852, 0.630144 and 0.153524 respectively, so b_1^2, b_2^2 and b_{12} have significance greater than 0.05, so they were omitted from the full model to generate a reduced model equation. The coefficients b_0, b_1 and b_2 were found to be significant at $P < 0.05$; hence, they were retained in the reduced model.

Table 3 *Ex vivo* drug diffusion study of all batches (F1–F9) ($n = 3$).

Time (h)	F1	F2	F3	F4	F5	F6	F7	F8	F9
0	0	0	0	0	0	0	0	0	0
1	1.03 ± 0.36	0.80 ± 0.31	0.91 ± 0.39	3.07 ± 0.27	2.09 ± 0.09	1.75 ± 0.08	2.71 ± 0.49	2.36 ± 0.36	2.02 ± 0.33
2	3.38 ± 0.37	2.99 ± 0.23	2.86 ± 0.64	6.41 ± 0.45	4.59 ± 0.60	3.83 ± 0.30	6.71 ± 0.66	4.36 ± 0.60	4.99 ± 0.39
3	6.11 ± 0.78	6.40 ± 0.44	5.56 ± 0.58	11.55 ± 0.70	8.68 ± 0.91	7.25 ± 0.29	12.79 ± 1.29	7.75 ± 0.94	10.38 ± 0.60
4	8.03 ± 1.09	9.48 ± 0.69	8.19 ± 1.42	15.74 ± 0.70	12.59 ± 0.86	10.51 ± 0.61	17.84 ± 1.17	12.78 ± 1.31	13.70 ± 0.84
5	13.46 ± 1.49	15.28 ± 0.13	13.61 ± 1.25	22.10 ± 0.83	18.97 ± 0.82	16.78 ± 0.74	24.43 ± 0.84	18.20 ± 1.49	20.21 ± 1.01
6	20.82 ± 0.79	22.84 ± 0.78	19.76 ± 1.06	29.34 ± 0.79	26.38 ± 0.74	24.34 ± 0.88	32.33 ± 1.53	26.13 ± 1.14	26.62 ± 0.89

Table 4 %EE of all batches (F1-F9) (n = 3).

Batch	Absorbance	Conc. (μg/ml)	Dilution factor	Conc. (mg/ml)	%EE
F1	0.9101 ± 0.0214	115.84 ± 3.34	100	11.584 ± 0.334	69.03 ± 1.99
F2	0.7831 ± 0.0188	99.76 ± 3.01	100	9.976 ± 0.301	59.45 ± 1.79
F3	0.4718 ± 0.0219	60.35 ± 3.40	100	6.35 ± 0.340	37.84 ± 2.03
F4	1.0381 ± 0.0403	132.04 ± 5.73	100	13.2 ± 0.573	78.66 ± 3.42
F5	0.8522 ± 0.0191	108.5 ± 3.05	100	10.85 ± 0.305	64.66 ± 1.82
F6	0.6111 ± 0.022	77.99 ± 3.42	100	7.799 ± 0.342	46.48 ± 2.04
F7	0.9978 ± 0.045	126.94 ± 6.33	100	12.69 ± 0.633	75.63 ± 3.77
F8	0.7901 ± 0.026	100.65 ± 3.92	100	10.065 ± 0.392	59.98 ± 2.34
F9	0.5511 ± 0.0118	70.39 ± 2.13	100	7.039 ± 0.213	41.95 ± 1.27

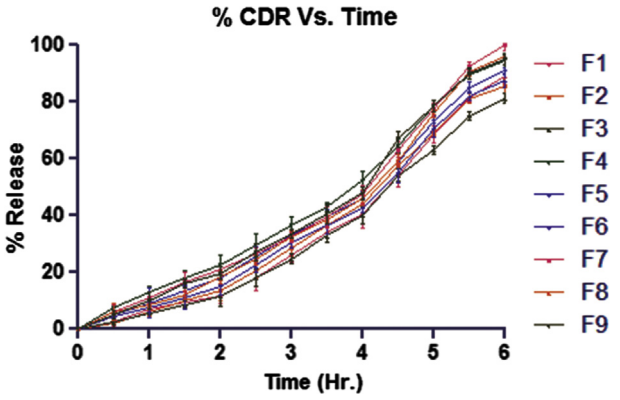

Figure 7 %Cumulative drug release of QTF with respect to time (n = 3).

3.4.2.2. Reduced model equation.

$$Y_2 = 90.74633 + 5.983833X_1 - 3.26283X_2 \quad (10)$$

So, from Eq. (10) of the reduced model, it can be qualitatively concluded that X_1 (5.983833) had the positive effect on the response of Y_2, which indicated that as the ratio of EPC to cholesterol increases, %CDR greatly increases. This is due to a surfactant property of EPC, it leads into increased diffusion of QTF across the cholesterol lipidic layer. Oppositely, as the number of sonication cycle decreases the %EE, also results in declining of %CDR.

3.4.3. Validation

The first checkpoint batch was prepared with CH: EPC molar ratio 1:2 and 2 sonication cycles by 80% amp of 2.5 min duration and checked for residual with F4 batch for entrapment efficiency. Similarly, the second checkpoint batch was prepared with CH: EPC molar ratio 1:2.5 and 2 sonication cycles by 80% amp of 2 min duration and checked for residual with F7 batch for % drug release.

The predicted value of %EE for checkpoint batch was 78.66 ± 3.42 of F4, and actual reading by three consecutive determinations was 73.03 ± 1.52, so residual was derived 5.63. Similarly, predicted value of %CDR for checkpoint batch was 99.66925 of F7, and actual reading by three consecutive determinations was 96.90 ± 1.88, so residual was derived 2.76925. It can be speculated from Table 6 that there is no significant difference in actual and predicted value of %EE and %CDR. So, we can conclude that our reduced model equation has good predictive power.

3.5. Release kinetic studies – release pattern and mechanism

Maximum goodness of fit value R^2 is observed 0.9941 for optimized batch F7 for Hopfenberg and Korsmeyer-Peppas than that of any other dissolution model. The Hopfenberg model suggests that drug release from surface eroding polymers so long as the surface area remains constant during the degradation process. Further that can be validated by performing Korsmeyer-Peppas modeling and finding value of release

Table 5 *In vitro* drug release study of all batches (F1–F9) (n = 3).

Time (h)	Cumulative % drug release (Q_{24})								
	F1	F2	F3	F4	F5	F6	F7	F8	F9
0	0	0	0	0	0	0	0	0	0
0.5	2.57 ± 1.6	2.0 ± 2.8	2.28 ± 2.8	7.67 ± 1.1	5.23 ± 1.3	4.37 ± 1.2	6.131 ± 2.6	5.89 ± 2.9	5.05 ± 1.4
1	6.75 ± 2.7	5.98 ± 1.5	5.72 ± 1.5	12.82 ± 2.4	9.18 ± 5.2	7.66 ± 1.9	11.047 ± 1.9	8.71 ± 1.2	9.972 ± 2.9
1.5	9.40 ± 1.8	9.85 ± 1.9	8.56 ± 1.2	17.77 ± 2.9	13.36 ± 1.6	11.16 ± 4.2	16.501 ± 3.6	11.93 ± 1.5	15.97 ± 1.7
2	11.47 ± 2.6	13.54 ± 3.6	11.7 ± 3.6	22.482 ± 3.7	17.98 ± 2.4	15.01 ± 3.1	20.78 ± 1.4	18.25 ± 2.3	19.57 ± 2.3
2.5	17.94 ± 4.6	20.37 ± 2.4	18.14 ± 2.9	29.464 ± 4.1	25.29 ± 3.6	22.37 ± 2.5	26.63 ± 2.1	24.27 ± 1.6	26.94 ± 3.1
3	26.03 ± 2.4	28.55 ± 3.0	24.7 ± 1.8	36.68 ± 2.6	32.97 ± 1.9	30.42 ± 1.8	32.35 ± 1.8	32.66 ± 1.9	33.27 ± 1.5
3.5	34.07 ± 3.5	36.72 ± 2.7	32.75 ± 2.5	43.05 ± 1.6	39.39 ± 2.7	36.50 ± 2.8	39.29 ± 3.8	38.71 ± 1.1	40.43 ± 3.5
4	40.40 ± 5.1	44.05 ± 1.8	39.98 ± 3.2	52.26 ± 3.3	46.07 ± 2.2	42.41 ± 1.4	47.42 ± 3.2	46.17 ± 2.6	47.83 ± 2.2
4.5	54.17 ± 4.3	57.39 ± 2.2	54.17 ± 2.1	64.49 ± 2.5	58.78 ± 3.8	55.13 ± 3.8	63.07 ± 2.7	59.08 ± 2.3	66.85 ± 2.8
5	68.42 ± 2.9	69.22 ± 1.0	62.96 ± 1.5	78.53 ± 1.2	72.75 ± 2.4	70.59 ± 2.9	77.45 ± 2.0	75.89 ± 1.3	78.49 ± 1.9
5.5	81.33 ± 1.5	81.15 ± 1.8	75 ± 1.3	89.67 ± 1.9	85.11 ± 1.7	81.75 ± 1.1	92.48 ± 1.3	90.36 ± 1.5	90.14 ± 2.1
6	88.81 ± 2.070	85.35 ± 2.42	81.11 ± 1.76	94.450 ± 2.22	91.116 ± 1.00	87.27 ± 2.12	99.920 ± 1.88	96.030 ± 1.11	95.223 ± 2.01

Table 6 Regression analysis and ANOVA for Y_1 and Y_2.

Regression statistics for Y_1	
Multiple R	0.997395
R Square	0.994798
Adjusted R square	0.986127
Standard error	1.712563
Observations	9

Anova

	DF	SS	MS	F	Significance F
Regression	5	1682.474	336.4947	114.7321	0.001268
Residual	3	8.798619	2.932873		
Total	8	1691.272			

Results of checkpoint batch

Predicted	Actual	Residual
74.95139	73.03 ± 1.52	1.92139

Regression statistics for Y_2

Multiple R	0.996687
R Square	0.993386
Adjusted R square	0.982362
Standard error	0.789968
Observations	9

ANOVA

	DF	SS	MS	F	Significance F
Regression	5	281.1798	56.23596	90.11458	0.001816
Residual	3	1.872148	0.624049		
Total	8	283.0519			

Results of checkpoint batch

Batch	Predicted	Actual	Residual
1	78.66	73.03 ± 1.52	5.63
2	99.66925	96.90 ± 1.88	2.76925

exponent. Value of n was found 1.561, indicated transport mechanism of the drug release follows supercase Case II. Supercase II mechanism generally refers to erosion of polymeric chain and anomalous transport (non-Fickian) refers to a combination of both diffusion and erosion controlled drug release and independent of a concentration gradient.

Generally release from liposomal lamella of lipophilic drugs follows zero order and Fickian mechanism of transport that release by concentration gradient in an isotonic solution. Simulated nasal fluid is slightly hypotonic to body fluids which results in its swelling and rupturing of liposomal sac. Moreover, at the body temperature of 37 °C, EPC get melted down (T_m of EPC is 20 °C); hence, liposomes get eroded. The drug entrapped in the layers of the lamella, is released by the diffusion mechanism. As the lamellar backbone of the cholesterol and lecithin degrades, the drug from the core of the liposomes is released by breakdown/ erosion mechanism.

3.6. Animal study

3.6.1. Gamma scintigraphy

The scintigraphy pictures in mice after intranasal administrations are demonstrated in Fig. 8. This obviously exhibits significant radioactivity aggregation in the brain after intranasal administration for a desired period and these results are in great concurrence with the past discoveries (Patil et al., 2010). Results of gamma scintigraphy study revealed that liposomal dispersion shows more accumulated TC^{99m} into the brain to compare to solution of TC^{99m}. Elevated TC^{99m} accumulation into the brain by liposomes confirms its efficiency of targeted delivery. Moderate amount of TC^{99m} into the lungs and respiratory tract through nasal route administration is observed as breathing in mice during nasal administration drags the dispersion into those tissues. From Study, it is clearly stated that, accumulation of ^{99m}Tc is more in the brain of intranasally given liposomes than that of the simple solution.

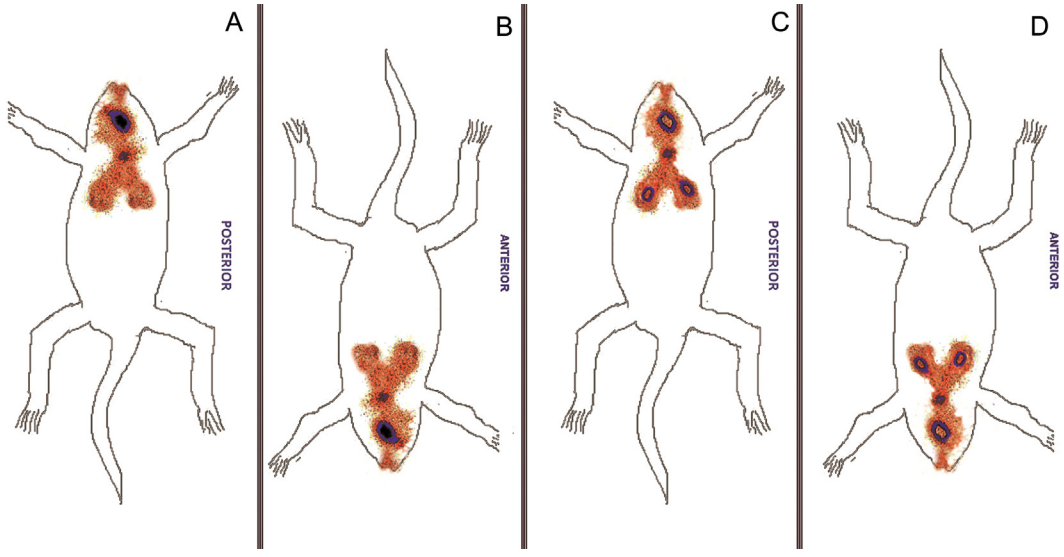

Figure 8 Gamma scintigraphy results after nasal administration of. A. QTF liposome (Posterior (A) and anterior (a)); B. QTF solution in mice (Posterior (B) and anterior (b)).

Table 7 QTF amount (ng/ml) into the brain homogenate after nasal administration ($n = 3$).

Time (hr)	QTF amount (ng/ml) into the brain	
	QTF dispersion	QTF liposomes
1	157.3333 ± 55.89574	85 ± 33.6006
2	191 ± 48.77499	177.6667 ± 39.8288
3	225.3333 ± 31.56475	255 ± 40.15
4	92.66667 ± 8.621678	221.6667 ± 8.144528
5	49.33333 ± 8.504901	116.3333 ± 18.037
6	21.66667 ± 8.736895	46 ± 12.16553

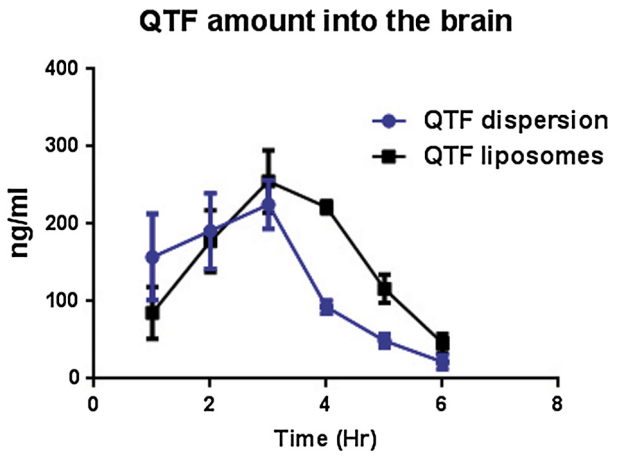

Figure 9 Amount of QTF in brain homogenate (ng/ml) containing liposome and simple dispersion ($n = 3$).

3.6.2. In vivo study

The brain:plasma amount for different formulations administered indicated that the brain:plasma ratio for QTF liposomes administered by intranasal route was significantly higher ($p < 0.05$, $n = 3$) in comparison with QTF dispersion as indicated in Table 7. Initially, the amount obtained by liposome was less than that obtained by the simple dispersion. But after that, in the second phase, the amount obtained for both dispersions was almost similar. And at the last, liposomes exceeded the availability of QTF in the mouse brain. QTF diffusion occurred at a constant rate of the dispersion, while for liposome, QTF diffusion gradually increased. That's why, though QTF diffusion was higher in dispersion in the first phase, at last phase diffusion by liposome was higher. These results support the existence of an alternative brain entry pathway for QTF by formulating in liposome by nasal route as indicated by rapid drug uptake obtained after intranasal administration of QTF liposome in comparison with QTF dispersion administered Fig. 9.

3.6.3. Nasal ciliotoxicity study

Nasal ciliotoxicity studies (Fig. 10) revealed that nasal mucosa treated with SNF pH 6.8 (negative control) showed intact epithelium layer without any necrosis while nasal mucosa treated with isopropyl alcohol (positive control mucociliary toxic agent) showed complete destruction of epithelium layer and necrosis and even the deeper tissue parts were also destroyed. QTF liposomes prepared in our studies did not exhibit any toxicity, as no change could be noticed in the gross morphology and histology of the nasal mucosa.

4. Conclusion

Liposomal formulation containing QTF was successfully formed using cholesterol and EPC using 3^2 factorial design. The maximum entrapment efficiency was observed in batch F4 which was prepared with 1:2 CH:EPC ratio and 2 cycles of sonication. There was an increase in entrapment efficiency to decrease with sonication cycles and increase in release with an increase in EPC ratio. The batch F7 was optimized based on dissolution study and evaluated for diffusion study. Results reveal that liposome had higher diffusivity than dispersion. *In vivo* and scintigraphy study proved that the formulation has better potential to deliver drugs to the brain than by the simple dispersion and solution. Higher brain uptake and distribution of QTF from liposomes for intranasal administration compared to simple dispersion indicated that the developed formulation can be a good platform for administration of drugs targeting the brain.

Declaration of interest

The authors report no declarations of interest.

Acknowledgements

The authors would like to thank L.J. Institute of Pharmacy, LJK trust, Ahmedabad and Dept. of Pharmaceutical Sciences, Saurashtra University, Rajkot for providing the needed lab facilities. The authors also thank Infocus Diagnostic Centre, Nuclear Medicine Department, Mithakhali, Ahmedabad for their kind support in mice gamma scintigraphy. The authors

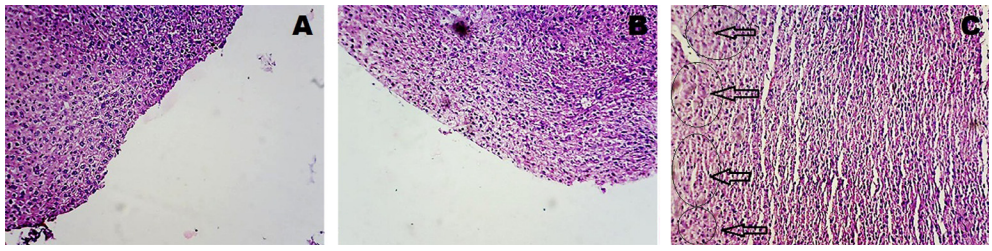

Figure 10 Photomicrographs of sheep nasal mucosa. A. Control; B. Nasal mucosa after diffusion study of liposomal formulation of QTF; C. Nasal mucosa treated with IPA.

express their gratitude to Vav Life sciences Pvt. Ltd., Mumbai for the generous gift of Egg Phosphatidylcholine.

References

Aacharya, S.P., Pundarikakshudu, K., Upadhyay, P., Shelat, P., Lalwani, A., 2015. Development of phenytoin intranasal microemulsion for treatment of epilepsy. J. Pharma. Invest. 45 (4), 375–384.

Abbott, N.J., Romero, I.A., 1996. Transporting therapeutics across the blood brain barrier. Mol. Med. 2, 106–113.

Afergan, E., Epstein, H., Dahan, R., Koroukhov, N., Rohekar, K., Danenberg, H.D., 2008. Delivery of serotonin to the brain by monocytes following phagocytosis of liposomes. J. Control. Release 132, 84–90.

Alsarra, I.A., Hamed, A.Y., Alanazi, F.K., 2008. Acyclovir liposomes for intranasal systemic delivery: development and pharmacokinetics evaluation. Drug Delivery 15 (5), 313–321.

Alsarra, I.A., Hamed, A.Y., Alanazi, F.K., Maghraby, G.M., 2010. Vesicular systems for intranasal drug delivery. In: Jain, K.K. (Ed.), Drug Delivery to the Central Nervous System, sixth ed. Springer Science & Business Media, pp. 175–203.

Arora, P., Sharma, S., Gary, S.S., 2002. Permeability issues in nasal drug delivery. Drug Discov Today. 7 (18), 967–975.

Arumugam, K., Subramanian, G.S., Mallayasamy, S.R., Averineni, R. K., Reddy, M.S., Udupa, N., 2008. A study of rivastigmine liposomes for delivery into the brain through intranasal route. Acta Pharm. 58 (3), 287–297.

Bamba, M., Puisieux, F., Marty, J.P., Carstensen, J.T., 1979. Release mechanisms in gel forming sustained release preparation. Int. J. Pharm. 2, 307–315.

Behl, C.R., Pimplaskar, H.K., Sileno, A.P., 1998. Effects of physicochemical properties and other factors on systemic nasal drug delivery. Adv. Drug Deliv. Rev. 29, 89–116.

Brayfield, A., Sweetman, S.C., 2007. Martindale, the Complete Drug Reference. Pharmaceutical Press, London.

Brgles, M., Jurasin, D., Sikirić, M.D., Frkanec, R., Tomasić, J., 2008. Entrapment of ovalbumin into liposomes-factors affecting entrapment efficiency, liposome size, and zeta potential. J. Liposome Res. 18 (3), 235–248.

Briuglia, M.L., Rotella, C., McFarlane, A., Lamprou, D.A., 2015. Influence of cholesterol on liposome stability and on in vitro drug release. Drug Deliv. Transl. Res. 5 (3), 231–242.

Chandaroy, P., Sen, A., Alexandridis, P., Hui, S.W., 2002. Utilizing temperature-sensitive association of pluronic F-127 with lipid bilayers to control liposome cell adhesion. Biochim. Biophys. Acta 1559 (1), 32–42.

Costantino, H.R., Illum, L., Brandt, G., Johnson, P.H., Quay, S.C., 2007. Intranasal delivery: physicochemical and therapeutic aspects. Int. J. Pharm. 337 (1–2), 1–24.

Fang, J.Y., Hwang, T.L., Huang, Y.L., 2009. Liposomes as vehicles for enhancing drug delivery via skin routes. Curr. Nanosci. 2 (1), 55–70.

Fielding, R.M., 1991. Liposomal drug delivery, advantages and limitations from a clinical pharmacokinetic and therapeutic perspective. Clin. Pharmacokinet. 21 (3), 155–164.

Freireich, E.J., 1966. Quantitative comparison of toxicity of anticancer agents in mouse, rat, dog, monkey and man. Cancer Chemother. Rep. 50 (4), 219–244.

Frey, W.H., 2002. Intranasal delivery: bypassing the blood-brain barrier to deliver therapeutic agents to the brain and spinal cord. Drug Deliv. Technol. 2, 46–49.

Garcia, E.G., Andrieux, K., Gilb, S., Couvreur, P., 2005. Colloidal carriers and blood–brain barrier (BBB) translocation: a way to deliver drugs to the brain. Int. J. Pharm. 298, 274–292.

Ghanbarzadeh, S., Valizadeh, H., Zakeri, P.M., 2013. Application of response surface methodology in development of sirolimus liposomes prepared by thin film hydration technique. Bioimpacts. 3 (2), 75–81.

Hamed, S.A., Mahmoud, A.A., Kamel, A.O., Hady, M.A., Gehanne, A.S.A., 2012. Phospholipid based colloidal poloxamer–nanocubic vesicles for brain targeting via the nasal rout. Colloids Surf. B 100 (1), 146–154.

Hildebrandt, I.J., Su, H., Weber, W.A., 2008. Anesthesia and other considerations for in vivo imaging of small animals. ILAR J. 49 (1), 17–26.

Hiromasa, N., Haruhisa, U., Masayuki, N., 1999. Effects of sonication on the lamellar structures of L-α-dipalmitoyl phosphatidylcholine (DPPC)/saccharide/water systems. Chem. Pharm. Bull. 47 (10), 1355–1362.

Illum, L., 2000. Transport of drugs from the nasal cavity to the central nervous system. Eur. J. Pharm. Sci. 11, 1–18.

Joseph, A.N., Zasadzinski, K., 1986. Transmission electron microscopy observations of sonication-induced changes in liposome structure, biophys. J. Biophys. Soc. 49, 1119–1130.

Jung, S.H., Seong, H., Cho, S.H., Jeong, K.S., Shin, B.C., 2009. Polyethylene glycol complexed cationic liposome for enhanced cellular uptake and anticancer activity. Int. J. Pharm. 382, 254–261.

Kararli, T.T., Needham, T.E., Griffin, M., Schoenhard, G., Ferro, L. J., Alcorn, L., 1992. Oral delivery of a renin inhibitor compound using emulsion formulations. Pharm. Res. 9, 888–893.

Laouini, A., Jaafar, M.C., Limayem, B.I., Sfar, S., Charcosset, C., Fessi, H., 2012. Preparation, characterization and applications of liposomes: state of the art. J. Colloid Sci. Biotechnol. 1, 147–168.

Lasic, D.D., Papahadjopoulos, D., 1995. Liposomes revisited. Science 267, 1275–1276.

Liu, J.J., Nazzal, S., Chang, T.S., Tsai, T., 2013. Preparation and characterization of cosmeceutical liposomes loaded with avobenzone and arbutin. J. Cosmet. Sci. 64 (1), 9–17.

Lohan, S., Sharma, S., Murthy, R.R., 2015. Formulation and evaluation of solid lipid nanoparticles of QTF and quetiapine hemifumarate for brain delivery in rat model. Pharm. Nanotechnol. 1 (3), 239–247.

Michel, A.D., Suzuki, K., 1985. Zeta potential of colloids in water and waste water. In: ASTM Standard D, American Society for Testing and Materials, vol. 44, pp. 4187–4282.

Misra, A., Ganesh, S., Shahiwala, A., Shah, S.P., 2003. Drug delivery to the central nervous system: a review. J. Pharm. Pharmaceut. Sci. 6 (2), 252–273.

Nill, B., 2003. Liposomes for Drug Delivery from Physico-chemical Studies to Applications. Acta Universitatis Upsaliensis, Uppsala.

Pardridge, W., 1999. Transport of small molecules through the blood-brain barrier: biology and methodology. Adv. Drug Deliv. Rev. 15, 5–36.

Parmar, H., Bhandari, A., Shah, D., 2011. Recent techniques in nasal drug delivery: a review. Int. J. Drug Develope. Res. 3 (1), 99–106.

Pathan, S.A., Zeenat, I., Zaidi, S.M.A., Talegaonkar, S., Vohra, D., Jain, G.K., Azeem, A., Jain, N., Lalani, J.R., Khar, R.K., Ahmad, F.J., 2009. CNS drug delivery systems: novel approaches. Recent Pat. Drug Deliv. Formulation 3, 71–89.

Patil, S., Babbar, A., Mathur, R., Mishra, A., Sawant, K., 2010. Mucoadhesive chitosan microspheres of carvedilol for nasal administration. J. Drug Target. 18, 321–331.

Pavia, D.L., Gary, M.L., Kriz, G.S., Vyvyan, J.A., 2008. Introduction to spectroscopy. In: Cole, B. (Ed.), Spectroscopy, second ed. Cengage Learning, pp. 26–107.

Rathod, S., Deshpande, S.G., 2010. Design and evaluation of liposomal formulation of pilocarpine nitrate. Indian J. Pharm. Sci. 72 (2), 155–160.

Reddy, S.P., Satyanarayana, P., Verma, K.K., Naga, R., Kumar, S., Sundaram, S.P., 2011. Novel reverse phase HPLC method devel-

opment and validation of quetiapine fumatrate in bulk and tablet dosage form. Int. J. Pharm. Int. Res. 1 (2), 95–99.
Sahu, D., Rana, A.C., 2011. Development of analytical method for quetiapine fumarate by UV spectrophotometry. Int. J. Res. Ayurveda Pharm. 2 (2), 588–591.
Santos, H.M., Lodeiro, C., 2009. The power of ultrasound. In: Capelo-Martínez, J.L. (Ed.), Ultrasound Chemistry: Analytical Applications, seventh ed. Wiley, New York, pp. 1–16.
Schnyder, S., Krahenbuhl, J., Drewe, J., Huwyler, S., 2005. Targeting of daunomycin using biotinylated immunoliposomes: pharmacokinetics, tissue distribution and in vitro pharmacological effects. J. Drug Target. 13, 325–335.
Senthilkumar, K.L., Ezhilmuthu, R.P., Praveen, P., 2012. Preparation and characterization of nabumetone liposomes. Int. J. LifeSci. Bt Pharm. Res. 1 (1), 81–86.
Shariat, S., Badiee, A., Jaafari, M.R., Mortazavi, S.A., 2014. Optimization of a method to prepare liposomes containing HER2/NEU- derived peptide as a vaccine delivery system for breast cancer. Iran J. Pharm. Res. 13, 15–25.
Shi, N., Zhang, Y., Zhu, C., Boado, R.J., Pardridge, W.M., 2001. Brain-specific expression of an exogenous gene after I.V. administration. Proc. Nat. Acad. Sci. 98, 12754–12759.
Thorne, R.G., Emory, C.R., Ala, T.A., Fery, W.H., 1995. Quantitative analysis of the olfactory pathway for drug delivery to the brain. Brain Res. 692 (1–2), 278–282.
Tomoko, N., Fumiyoshi, I., 2005. Encapsulation efficiency of water-soluble and insoluble drugs in liposomes prepared by the microencapsulation vesicle method. Int. J. Pharm. 298 (1), 198–205.
Türker, S., Onur, E., Özer, Y., 2004. Nasal route and drug delivery systems. Pharm. World Sci. 26, 137–142.
Ugwoke, M.I., Verbek, N., Kinget, R., 2001. The biopharmaceutical aspects of nasal mucoadhesion drug delivery. J. Pharm. Pharmacol. 53, 3–22.
Vincenzo, P., Roberto, M., Anna, F., Sandra, F., 2003. Quality control of commercial tablets containing the novel antipsychotic quetiapine. J. Pharm. Biomed. Anal. 32, 1037–1044.
Vyas, S.P., Goswami, S.K., Singh, R., 1995. Liposomes based nasal delivery system of nifedipine: development and characterization. Int. J. Pharm. 118 (1), 23–30.
Watts, L.P., Fisher, A.N., Norbury, H.M., Gill, J.H., Nankervis, I.R., Davis, S.S., 2002. Intranasal delivery of morphine. J. Pharmacol. Exp. Ther. 301, 391–400.
Woensel, M., Wauthoz, N., Rosière, R., Amighi, K., Mathieu, V., Lefranc, F., Gool, S.W., Vleeschouwer, S., 2013. Formulations for intranasal delivery of pharmacological agents to combat brain disease: a new opportunity to tackle GBM? Cancers 5, 1020–1048.
Xie, Y., Ye, L., Zhang, X., Cui, W., Lou, J., Nagai, T., 2005. Transport of nerve growth factor encapsulated into liposomes across the blood-brain barrier: in vitro and in vivo studies. J. Control. Release 105, 106–119.